

## ***Enhanced Direct Major Histocompatibility Complex Class I Self-Antigen Presentation Induced by Chlamydia Infection***

The Faculty of Oregon State University has made this article openly available.  
Please share how this access benefits you. Your story matters.

<b>Citation</b>	Cram, E. D., Simmons, R. S., Palmer, A. L., Hildebrand, W. H., Rockey, D.D., & Dolan, B. P. (2016). Enhanced direct major histocompatibility complex class I self-antigen presentation induced by Chlamydia infection. <i>Infection and Immunity</i> , 84(2), 480 –490. doi:10.1128/IAI.01254-15
<b>DOI</b>	10.1128/IAI.01254-15
<b>Publisher</b>	American Society for Microbiology
<b>Version</b>	Version of Record
<b>Terms of Use</b>	<a href="http://cdss.library.oregonstate.edu/sa-termsfuse">http://cdss.library.oregonstate.edu/sa-termsfuse</a>

# Enhanced Direct Major Histocompatibility Complex Class I Self-Antigen Presentation Induced by *Chlamydia* Infection

Erik D. Cram,<sup>a</sup> Ryan S. Simmons,<sup>a</sup> Amy L. Palmer,<sup>a</sup> William H. Hildebrand,<sup>b</sup> Daniel D. Rockey,<sup>a</sup>  Brian P. Dolan<sup>a</sup>

Department of Biomedical Sciences, College of Veterinary Medicine, Oregon State University, Corvallis, Oregon, USA<sup>a</sup>; Department of Microbiology and Immunology, University of Oklahoma Health Sciences Center, Oklahoma City, Oklahoma, USA<sup>b</sup>

The direct major histocompatibility complex (MHC) class I antigen presentation pathway ensures intracellular peptides are displayed at the cellular surface for recognition of infected or transformed cells by CD8<sup>+</sup> cytotoxic T lymphocytes. *Chlamydia* spp. are obligate intracellular bacteria and, as such, should be targeted by CD8<sup>+</sup> T cells. It is likely that *Chlamydia* spp. have evolved mechanisms to avoid the CD8<sup>+</sup> killer T cell responses by interfering with MHC class I antigen presentation. Using a model system of self-peptide presentation which allows for posttranslational control of the model protein's stability, we tested the ability of various *Chlamydia* species to alter direct MHC class I antigen presentation. Infection of the JY lymphoblastoid cell line limited the accumulation of a model host protein and increased presentation of the model-protein-derived peptides. Enhanced self-peptide presentation was detected only when presentation was restricted to defective ribosomal products, or DRiPs, and total MHC class I levels remained unaltered. Skewed antigen presentation was dependent on a bacterial synthesized component, as evidenced by reversal of the observed phenotype upon preventing bacterial transcription, translation, and the inhibition of bacterial lipooligosaccharide synthesis. These data suggest that *Chlamydia* spp. have evolved to alter the host antigen presentation machinery to favor presentation of defective and rapidly degraded forms of self-antigen, possibly as a mechanism to diminish the presentation of peptides derived from bacterial proteins.

Activated cytotoxic CD8<sup>+</sup> T lymphocytes are responsible for directly killing self-cells which have become infected or transformed. In order to initiate killing, the T cell receptors (TCRs) expressed on the surfaces of CD8<sup>+</sup> T lymphocytes must recognize a specific antigenic peptide bound to a major histocompatibility complex (MHC) class I molecule expressed on the target cell. Because the peptide is the lynchpin in the entire immune reaction, an understanding of how cells directly process and present peptides is of utmost importance if we are to exploit the T cell response to eliminate chronically infected cells or tumors.

Bacteria of the genus *Chlamydia* are obligate intracellular organisms and as such, they should be subject to control by CD8<sup>+</sup> T cells. Indeed, peptides derived from chlamydial proteins are known to be presented by MHC class I molecules (reviewed in reference 1) and *Chlamydia*-reactive CD8<sup>+</sup> T cells have been detected in patients (2, 3). Despite the presence of antigen-specific T cells, infection with *Chlamydia trachomatis* can cause serious diseases in humans. Clinical signs and long-term consequences of *C. trachomatis* infection particularly afflict women and include pelvic inflammatory disease, ectopic pregnancy, premature birth, hydrosalpinx, and infertility (4). Often, intracellular pathogens have evolved a multitude of ways to evade CD8<sup>+</sup> T cell responses by altering the MHC class I antigen presentation pathway (5, 6). Indeed, infection with different *Chlamydia* species can decrease the cell surface levels of MHC class I molecules, suggesting immune evasion of CD8<sup>+</sup> T cell responses (7–9). As the field advances toward the development of a successful vaccine, it is imperative to determine what, if any, mechanisms are used by *Chlamydia* species to alter antigen presentation.

Peptides directly presented on MHC class I molecules can be derived from any source of endogenous proteins, including self-peptides liberated from the parental protein as part of the normal process of protein turnover or from proteins rendered defective by any number of processes within the cell. Viruses, including HIV

(10), measles virus (11), influenza virus (12), and respiratory syncytial virus (13), often alter the self-peptide repertoire on MHC class I molecules. Changes in cellular metabolic activity can also skew the repertoire of self-peptides displayed at the cell surface (14). Since CD8<sup>+</sup> T cells can react to self-antigens, the changes in peptide repertoire may have implications in autoimmune disorders. It is therefore instructive to think not only of foreign antigen presentation but also of alterations in self-peptide presentation resulting from intracellular pathogen infection.

We report here that during chlamydial infections host cells increase the presentation of self-peptides while simultaneously decreasing levels of a model host protein. The loss of self-protein was neither due to proteasome-mediated decay nor due to a decrease in the level of mRNA transcripts, suggesting that a bacterial synthesized component altered the host protein's ability to accumulate within the cell. The resulting increase in self-peptide presentation may explain the association of autoimmune disease and chlamydial infections (15, 16). Furthermore, enhancing self-peptide presentation may mask chlamydial infection by decreasing the presentation efficiency of chlamydial peptides.

Received 5 October 2015 Returned for modification 26 October 2015

Accepted 17 November 2015

Accepted manuscript posted online 23 November 2015

Citation Cram ED, Simmons RS, Palmer AL, Hildebrand WH, Rockey DD, Dolan BP. 2016. Enhanced direct major histocompatibility complex class I self-antigen presentation induced by *Chlamydia* infection. *Infect Immun* 84:480–490. doi:10.1128/IAI.01254-15.

Editor: C. R. Roy

Address correspondence to Brian P. Dolan, brian.dolan@oregonstate.edu.

E.D.C. and R.S.S. contributed equally to this article.

Copyright © 2016, American Society for Microbiology. All Rights Reserved.

## MATERIALS AND METHODS

**Cell lines, antibodies, and reagents.** The human B lymphoblastoid cell line JY (17) and the epithelial tumor cell line MCF7 were cultured in RPMI 1640 medium (Gibco) supplemented with 7.5% fetal calf serum (Atlanta Biological), GlutaMAX (Gibco, 20 mM), and HEPES (Gibco, 10 mM). Cells were cultured in a humidified incubator at 37°C with 6% CO<sub>2</sub>. The monoclonal antibody (MAb) RL15A (anti-HLA-A2-SVG, described previously [18]) was labeled with an Alexa Fluor 647 kit (Molecular Probes), and the fluorescence to protein (F/P) ratio was determined according to manufacturer directions. The MAb W6/32 (anti-HLA-A,B,C) was used as previously described (17). Goat polyclonal anti-green fluorescent protein (GFP) antibody and recombinant GFP were from Novus. The proteasome inhibitor epoxomicin (Enzo) was used at a concentration of 1 µg/ml. Emetine (MP Pharmaceuticals) was used at a concentration of 10 µM. The protein transport inhibitor brefeldin A (BFA; MP Pharmaceuticals) was used at a concentration of 10 µM. The human Toll-like receptor (TLR) agonist kit was from InvivoGen. Shield-1 (Clontech) was used at a concentration of 1 µg/ml unless otherwise indicated.

**SCRAP-SVG construct and transfections.** SCRAP-SVG was constructed as follows. The FKB12 destabilization domain was amplified from pCAGGS/SCRAP (19) using the forward primer 5'-TCTAGAGAGCTCCACCATTGGGAGTGCAGGTGGAAACCA-3' (primer 1) and the reverse primer 5'-AAGTGGAGTGAACACCCCTCCAAGTATCCGGTTTAGAAGTCC-3' (primer 2). Venus was amplified from pSC11-VFP-Ub-RGY (20) using the forward primer 5'-TCAGTTGGAGGGGTGTTACACCTCAGTTGTGAGCAAGGGCGAGGAG-3' (primer 3) and the reverse primer 5'-AGATCTCTCGAGTTACTTGACAGCTCGTCCATGCCGAG-3' (primer 4). PCR products were collected using a Qiagen PCR purification kit. Purified amplicons were then used as the templates in a zipper PCR using primers 1 and 4. The resultant PCR product was purified, digested with SacI and XhoI, and cloned into the pCAGGS vector. PvuI-digested plasmid DNA was ethanol purified and resuspended in H<sub>2</sub>O. The linearized plasmid DNA was mixed with 10<sup>5</sup> JY cells in Amaxa SF solution. JY cells were electroporated with the Amaxa shuttle nucleofector (program DS-138). Cells were cultured for 1 week and exposed to Shield-1 overnight. The following day, Venus fluorescent protein-positive (VFP<sup>+</sup>) cells were sorted with a BD FACSAria II and cultured with antibiotics (penicillin-streptomycin and gentamicin, all from Gibco) for 10 days to prevent contamination. A second round of fluorescence-activated cell sorting (FACS) was necessary to achieve >95% VFP<sup>+</sup> cells. For transient transfection, 5 × 10<sup>5</sup> MCF7 cells were mixed with 500 ng of the pCAGGS-SCRAP-SVG vector in 20 µl of transfection solution SF (Lonza) and transfected with the Amaxa shuttle nucleofector (program FF-120).

**Antigen presentation assays.** JY cells were harvested and cultured at 10<sup>6</sup> cells/ml for various times and with various compounds before harvesting. For kinetic experiments, cells were harvested and kept at 4°C until the end of the assay, when all samples were stained and analyzed together. In some experiments, cells were washed in ice-cold citric acid buffer (pH 3) for 2 min (21); the cells were then washed and resuspended in culture medium at 10<sup>6</sup> cells/ml. After cell harvesting, the cells were washed in 0.1% bovine serum albumin-Hanks balanced salt solution and labeled with Alexa Fluor 647-coupled RL15A MAb or W6/32 at 4°C for 30 min. The cells were then washed, and W6/32-labeled cells were stained with DyLight 649 goat-anti-mouse IgG for 30 min at 4°C. After being washed to remove excess antibody, the cells were analyzed by flow cytometry using a BD Accuri C6 flow cytometer. For kinetic analysis, single data points were analyzed. When single time points were analyzed, a minimum of three individual cell stains were included. Data analysis was completed with Accuri software. Single-color controls were used to ensure proper color compensation. Each iteration of an antigen presentation experiment was repeated a minimum of three times.

**Chlamydia strains and cell lines.** McCoy cells were grown in minimal essential medium (Life Technologies) with 10% fetal bovine serum (Life Technologies). *Chlamydia trachomatis* serovar L2 transformed with mCherry plasmid, L2/pBRmChE (here L2-RFP, kindly provided by Rob-

ert J. Suchland, University of Washington), *C. trachomatis* D/UW-3, and *C. caviae* were propagated in McCoy cells. For all figures, *C. trachomatis* refers to the L2 serovar unless otherwise noted. Titers of chlamydial stocks were determined by counting the number of inclusion-forming units (IFU) per ml in JY cells. Chlamydial growth kinetics were established by infecting JY cells, and at different time points, cells were removed into a new 1.5-ml tube, centrifuged, and resuspended in phosphate-buffered saline (PBS). Lysing matrix C beads (MP Biomedicals) were added to each tube, which were then vortexed vigorously for 30 s. Samples were then centrifuged at 20,000 relative centrifugal force (RCF) for 10 min, and the supernatant was transferred to a new 1.5-ml tube and stored at -80°C. McCoy cells were then grown to confluence in a 24-well tray. Three serial dilutions were made from each sample and used to infect each monolayer in triplicate. The numbers of inclusion-forming units per ml were determined on monolayers fixed with methanol at 48 h postinfection (hpi).

**Infection and antigen presentation assays.** A total of 5 × 10<sup>5</sup> JY/SCRAP-SVG cells were centrifuged at 200 RCF for 5 min. The medium was removed, and the cells were resuspended in PBS (pH 7.4). The cells were then aliquoted into individual wells of a 24-well tissue culture plate in 400 µl of PBS. *Chlamydia* spp. were added to the cells, and the plate was centrifuged at 980 RCF for 1 h. After infection, 1 ml of RPMI medium supplemented with 2% L-glutamine and 10% FBS was added to each well. At 12 hpi, Shield-1 was added to the appropriate wells at a final concentration of 1.0 µM. The cells were incubated at 37°C in 6% CO<sub>2</sub> for 24 h. Unless otherwise noted, a multiplicity of infection (MOI) of 0.3 was used and was determined by measuring percentage of red fluorescent protein-positive (RFP<sup>+</sup>) cells by FACS analysis (see Fig. 2). For the kinetics assays, cells were resuspended in PBS and fixed, and the Venus fluorescent protein (VFP) was determined by flow cytometry at each time point. In some experiments, chloramphenicol (CAM; Sigma, 1.5 µg/ml), rifampin (RIF; Sigma, 10 ng/ml), or LPC-011 (LPC [kindly provided by Pei Zhou and Raphael Valdivia], 1.92 µg/ml) was added to cells during and after the infection and maintained in culture throughout the remainder of the experiment. In other experiments, epoxomicin (Enzo, 1 µg/ml) or BFA (MP Pharmaceuticals, 10 µM) was added to cells at approximately 17 hpi. Antigen presentation assays were performed as described above. For infection of MCF7 cells, after a 2-h incubation period posttransfection, the cells were infected with *C. trachomatis* D/UW-3 as described above. Prior to staining with RL15A, at 30 hpi, all medium was removed, and the monolayer was disrupted by treatment with 0.25% trypsin-EDTA (Life Technologies) and neutralized with RPMI. At 24 hpi, *C. caviae*-infected JY cells were washed with PBS and resuspended in 0.1 µM C6-NBD-ceramide (Invitrogen) for 1 h at 37°C. The cells were then centrifuged at 200 RCF, and the supernatant was aspirated and replaced with fresh RPMI. After a 3-h incubation period at 37°C, the cells were fixed in 4% paraformaldehyde and analyzed by fluorescence-activated cell sorting (FACS). Each antigen presentation assay was repeated a minimum of three times.

**Electron microscopy.** JY cells were infected at an MOI of 0.3, and at 24 hpi, cells were harvested and washed two times with Dulbecco's phosphate-buffered saline (DPBS) and resuspended in 1 ml of EM fixative A (2.5% glutaraldehyde, 1% paraformaldehyde, 0.1 M sodium cacodylate). Cells were submitted to the Oregon State University Electron Microscopy facility for thin sectioning and imaging with a FEI-Titan 80-200 in STEM mode. Approximately 100 cells were examined.

**Fluorescence microscopy.** JY cells infected with *C. trachomatis* L2-RFP or mock infected were harvested and washed with excess PBS and fixed with 4% paraformaldehyde as described above. Cells were then mixed with VectaShield (Vector Laboratories) containing DAPI (4',6'-diamidino-2-phenylindole; Sigma-Aldrich) to stain DNA and imaged with a Leica DML fluorescent scope with Chroma 49004 TRITC (tetramethyl rhodamine isothiocyanate) and 49021 DAPI filters. Ten fields were examined with a 100× oil immersion lens for RFP/DAPI, and images were taken with Retiga 2000R camera and QCapture Pro 6.0 software. A minimum of 10 fields (representing almost 50 cells) were examined.

**Quantification of SCRAP-SVG transcripts.** Three wells containing  $5 \times 10^5$  JY/SCRAP-SVG cells were either infected with L2-RFP or mock infected and then cultured for 24 h. RNA was extracted with the NucleoSpin RNA isolation kit (Clontech), and RNA was stored at  $-20^\circ\text{C}$ . Synthesis of cDNA from RNA extracts was performed using the RNA to cDNA EcoDry Premix (Clontech). For quantitative PCR (qPCR), a Fast SYBR green master mix (Life Technologies) was used with FKBP12 cloning primers 1 and 2, as mentioned above, with an input of  $1 \mu\text{l}$  of cDNA template for each reaction, repeated in triplicate. Transcript levels of SCRAP-SVG were normalized with ACTB amplicons generated from ACTB primers F 5'-ATCCTGCGTCTGGACCCTG-3' and R 5'-TAGCTCTTCTCCAGGGA-3'. Plasmids containing either SCRAP-SVG or ACTB were made into 10-fold serial dilutions ranging from  $10^3$  to  $10^{10}$  to serve as standards. ABI StepOne real-time PCR machine and StepOne software determined the transcript level of ACTB and SCRAP-SVG transcripts based on their abundance interpolated from each respective standard curve. Both biological and technical replicates were done in triplicate.

**Quantification of chlamydial genome copies.** In a 24-well tray, eight wells of McCoy cells were set to full confluence and infected with *C. trachomatis* L2-RFP as described above. Dulbecco's modified minimal essential medium (DMEM) containing either dimethyl sulfoxide (DMSO) or  $1.92 \mu\text{g/ml}$  LPC-011 was added to each well. At each time point, medium was removed, and the cells were washed in PBS. After the removal of the PBS,  $200 \mu\text{l}$  of sterile, nuclease-free water was added, and the cells were incubated for 5 min at  $37^\circ\text{C}$ . The cells were then lifted from the plate by gently pipetting and then stored at  $-80^\circ\text{C}$ . Dithiothreitol (DTT) was added to a final concentration of 5 mM, and the samples were heated to  $95^\circ\text{C}$  for 1 h. DNA was then extracted by using the DNeasy blood and tissue kit (Qiagen) according to the manufacturer's recommendations. Quantitative PCRs were set up using TaqMan Universal master mix (Life Technologies) and *C. trachomatis ompA* primers as previously described (22). The experiment was repeated three times.

**Quantitative Western blotting, quantitative flow cytometry, and efficiency calculations.** Cells were harvested and pellets were resuspended in SDS protein gel loading buffer (Amresco) with DTT at  $10^7$  cells/ml. The cells were lysed at  $95^\circ\text{C}$  for 30 min, with occasional vortexing. SDS-PAGE was performed with cell lysates using the Bolt electrophoresis system, followed by blotting onto nitrocellulose membranes using the iBlot 2 (Invitrogen). Membranes were blocked in 5% nonfat dehydrated milk, probed with primary antibodies, and incubated with secondary antibodies (LI-COR, IR Dye donkey-anti-goat 680 or 800). A goat polyclonal antibody recognizing a conserved peptide sequence present in both GFP and VFP was used to allow for direct quantification of VFP present in the cell lysate. Membranes were imaged with an Odyssey infrared imager (LI-COR). Intensity of the recombinant GFP standards was determined using LI-COR image studio software, and the resulting standard curve was used to quantify SCRAP-SVG accumulation in samples. The calculated molarity of VFP in the cell lysate was first converted to molecules/volume and then divided by the cell equivalents present in the lysate to determine the molecules/cell. Quantification of peptide-MHC complexes (pMHCs) was done according to previously published methods (23, 24). Alexa 647-coupled MEF beads were purchased from Bangs Laboratories and included in the FACS analysis. The standard curve generated was then used to determine the number of molecules of dye bound to the cell, and this number was divided by the F/P ratio of Alexa 647-coupled RL15A to determine the number of antibodies bound to the cell surface. The efficiency of antigen presentation was subsequently calculated by dividing the number of peptide-MHC complexes generated by the number of SCRAP-SVG molecules degraded. The results of five independent experiments are reported.

**Statistics.** Linear regressions, analyses of variance (ANOVAs), and *t* tests were performed using Prism software (GraphPad).

## RESULTS

MAbs with TCR-like specificity (known as TCRms) are a useful tool for quantifying MHC class I presentation of a particular peptide. We have recently used one such TCRm to determine that the efficiency of presentation of a peptide from a model self-protein was nearly 10 times greater than when the same model antigen was expressed by an infecting virus, suggesting that the source of the peptide was an important factor for efficient antigen presentation (19). We developed a new version of our original model protein (21) for studying the presentation of peptides via human MHC class I molecules. The model protein (Fig. 1A) contains a destabilization domain derived from the FKBP12 protein, which facilitates rapid degradation of the mosaic target protein. This process can be reversed by the addition of a small, cell-penetrating molecule termed Shield-1 (25). Sandwiched between the destabilization domain and Venus fluorescent protein (VFP), which acts as a reporter for the presence of a functional protein, is the peptide SVGGVFTSV (referred to here as SVG) derived from West Nile virus E protein, which can be presented by the human MHC class I molecule HLA-A2. We have previously described a similar model protein termed SCRAP (shield-controlled recombinant antigen protein) (17, 21). We refer to our new construct as SCRAP-SVG. The human lymphoblastoid cell line JY was transfected with SCRAP-SVG, and cells with a stable integration of SCRAP-SVG were selected based on VFP fluorescence signal in the presence of Shield-1. Compared to the parental cells, JY/SCRAP-SVG cells express low levels of VFP, but the addition of Shield-1 greatly increases VFP signal (Fig. 1B). HLA-A2-SVG complexes can be detected using the TCRm RL15A (18), and a representative staining of JY and JY/SCRAP-SVG cells shows increased RL15A staining in the stable transfectants (Fig. 1B). The accumulation of VFP was dose dependent, and saturation of the system was achieved with a dose of  $1.0 \mu\text{M}$  (Fig. 1C).

The kinetics of antigen presentation were measured in JY/SCRAP-SVG cells. Cells were first washed in a mild citric acid solution to strip existing peptide-MHC complexes from the cell surface and then cultured in the presence or absence of Shield-1. Recovery of HLA-A2-SVG complexes occurred rapidly and was blocked by drugs known to inhibit MHC class I antigen presentation, such as brefeldin A (BFA), which blocks the transport of MHC class I molecules through the endoplasmic reticulum, or emetine, which prevents protein synthesis (Fig. 1D and E). When cells were cultured in the presence of  $1.0 \mu\text{M}$  Shield-1 after acid stripping, HLA-A2-SVG complexes were still generated and detected at the cell surface, although in reduced number compared to results for cells treated with ethanol alone (Fig. 1D). However, the level of HLA-A2-SVG complexes generated in the presence of Shield-1 was significantly greater than that seen with treatment with either BFA or emetine (Fig. 1E). We and others have previously observed this phenomenon, and the data suggest that some inherently destabilized form of newly synthesized SCRAP-SVG is degraded and presented, despite the presence of a saturating dose of Shield-1 (17, 21, 26). This meets the definition of a defective ribosomal product (DRiP) (27), which are important sources of peptides for the antigen presentation pathway (28, 29). These data demonstrate that JY/SCRAP-SVG cells can be used to monitor host protein synthesis and antigen presentation.

Not all cell types can be infected with various *Chlamydia* species. To determine whether the JY cell line was susceptible to in-

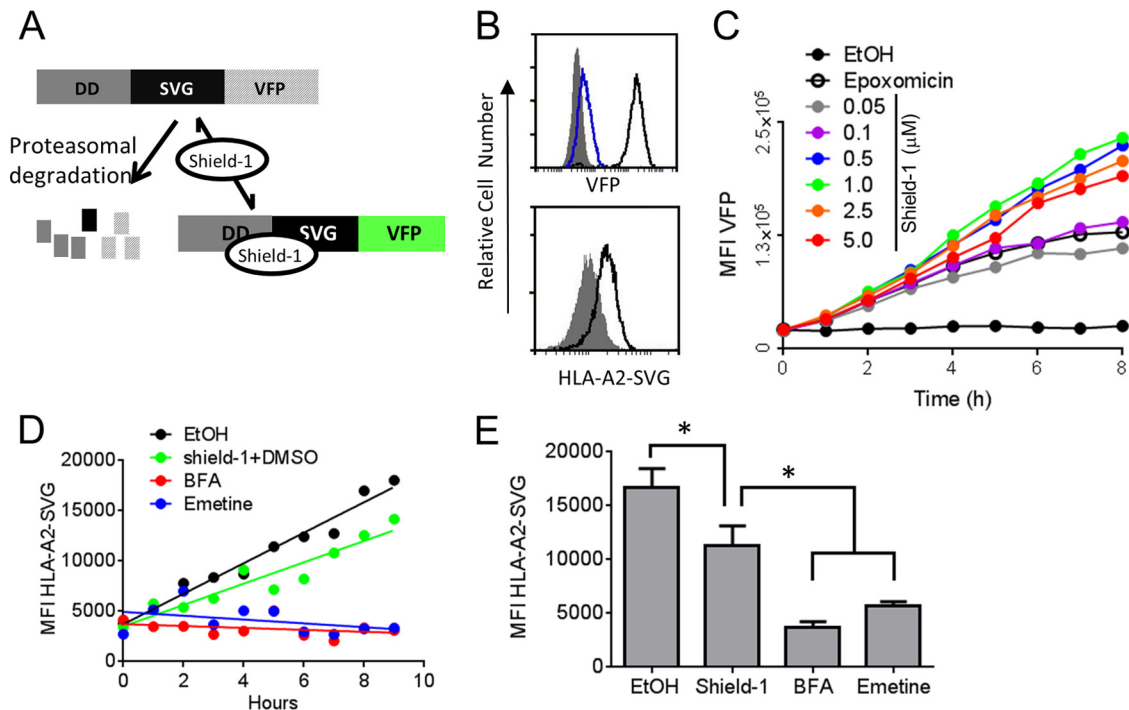


**FIG 1** Stabilization and presentation of SCRAP-SVG in JY cells. (A) Depiction of SCRAP-SVG, including the destabilization domain (DD), the SVG peptide, and VFP. In the absence of Shield-1, SCRAP-SVG is degraded by the proteasome. The addition of Shield-1 allows SCRAP-SVG to fold and gain fluorescence. (B) Flow cytometry histograms depicting VFP fluorescence of parental JY cells (shaded), JY/SCRAP-SVG cells treated with Shield-1 (black histogram), and JY/SCRAP-SVG cells treated with ethanol alone (blue trace). RL15A-stained JY/SCRAP-SVG cells (bottom histogram, black trace) and parental JY cells (shaded histogram) are used to measure HLA-A2-SVG complexes at the cell surface. (C) Dose response of JY/SCRAP-SVG cells with various concentrations of Shield-1 or epoxomicin, measuring the mean fluorescence intensity (MFI) of VFP fluorescence. (D) JY/SCRAP-SVG cells were washed in citric acid and cultured with ethanol (EtOH), 1  $\mu$ M Shield-1, BFA, or emetine and harvested at the indicated times for RL15A staining. (E) The same as in panel D except the cells were harvested at 8 h and stained in triplicate. Results for Shield-1-treated cells are statistically significantly different from results for ethanol-treated and either BFA- or emetine-treated cells (\*,  $P < 0.05$ ).

fection, we took advantage of a recombinant *C. trachomatis* serovar L2 strain expressing the mCherry red fluorescent protein (RFP). Electron microscopy analysis demonstrated that infected cells underwent a classical development cycle, represented by large inclusions harboring elementary bodies and reticulate bodies (Fig. 2A). Fluorescence microscopy analysis confirmed the presence of RFP in the infected cells only (Fig. 2B). Cells were also analyzed by flow cytometry for RFP expression (Fig. 2C), which has the advantage of quantifying infected and uninfected cells. We demonstrate that RFP detected in infected cells is newly synthesized by the bacteria and not introduced to the cells during infection, since treatment with the bacterial protein synthesis inhibitor chloramphenicol (CAM) prevented RFP expression during infection (Fig. 2D). In addition, we were able to infect JY/SCRAP-SVG cells with a distantly related chlamydial species, *C. caviae*, and quantify infection using fluorescent C6-NBD-ceramide (22), which is recruited to the chlamydial inclusion (Fig. 2E). *C. trachomatis* can also be recovered from infected cells and used to initiate another round of infection, demonstrating that *C. trachomatis* can complete its replication cycle in JY cells (Fig. 2F). Therefore, JY cells are susceptible to chlamydial infections.

To determine what effect chlamydial infection has on host-protein synthesis and antigen presentation, we infected JY/SCRAP-SVG cells with either RFP-expressing *C. trachomatis* serovar L2 or *C. caviae* and monitored accumulation of VFP in the presence of Shield-1, added 12 hpi. VFP levels initially increased in *C. trachomatis*-infected cells, but began to plateau at 14 to 16 hpi,

while a continued increase in VFP fluorescence was detected in uninfected cells (Fig. 3A). Examination of cells infected with either chlamydial strain showed a similar, statistically significant decrease in VFP levels 24 hpi (Fig. 3B). The loss of VFP fluorescence did not result from a decrease in SCRAP-SVG transcripts since transcript levels determined by qPCR analysis of cDNA prepared from infected cells were not significantly lower than those for uninfected cells (Fig. 3C). In addition to monitoring VFP kinetics, we also examined HLA-A2-SVG complex levels in infected cells. Because repeated harvesting and exposure to low pH necessary to acid strip existing peptide-MHC complexes from cells have the potential to impact chlamydial infection, we monitored levels of peptide-MHC complexes 12 h after the addition of Shield-1 (Fig. 3D). Treatment with BFA caused levels of HLA-A2-SVG to fall over a 12-h treatment period. Similar to data shown in Fig. 2, treatment with Shield-1 resulted in lower levels, but not a complete loss, of HLA-A2-SVG complexes, since only DRiP-derived substrates were replacing peptide-MHC complexes lost as a function of time due to normal protein turnover (Fig. 3D). Results were statistically significant ( $P < 0.05$  for the Student *t* test;  $P < 0.001$  for ANOVA). Infection of JY/SCRAP-SVG cells with *C. trachomatis* or *C. caviae* did not alter the levels of HLA-A2-SVG complexes when cells were treated with ethanol alone (Fig. 3E,  $P < 0.001$ , ANOVA), nor were total levels of MHC class I molecules altered (Fig. 3F) upon infection. However, treatment with Shield-1 led to an increase in peptide presentation over results for mock-infected cells (Fig. 3E,  $P < 0.05$ , Student *t* test). Because

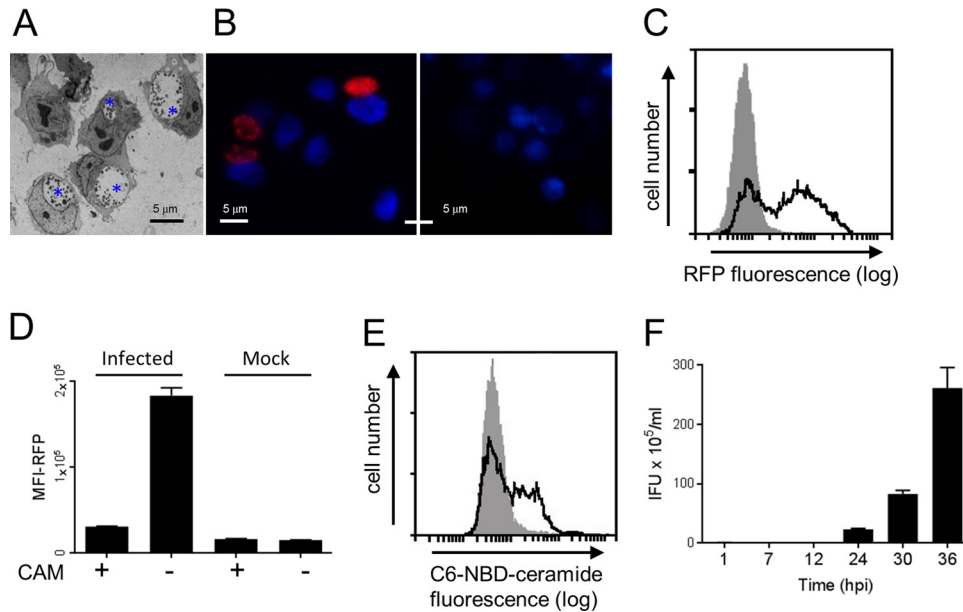


**FIG 2** *Chlamydia* species can successfully infect JY cells. (A) Electron micrograph of JY cells 24 h after infection with *C. trachomatis*. Blue asterisks show locations of *C. trachomatis* inclusions. (B) Fluorescence microscopy image of JY cells infected (left) or not infected (right) with RFP-expressing *C. trachomatis*. Cells were stained with DAPI to delineate nucleic acid. (C) RFP expression of *C. trachomatis*-infected JY cells (black trace) and uninfected cells (shaded histogram) analyzed by flow cytometry. (D) CAM was added to either infected or mock-infected cells, and the MFI of RFP fluorescence was recorded at 24 hpi. (E) JY cells were infected with *C. caviae* (black trace) or mock infected (shaded histogram) and identified by staining cells with C6-NBD-ceramide. (F) *C. trachomatis*-infected JY cells were harvested at the indicated times postinfection and disrupted, and the supernatants were used to infect McCoy cells. The infectious dose at each time point is plotted.

treatment with Shield-1 restricts presentation to DRiP substrates, these data suggest that *C. trachomatis* infection enhances the presentation of self-peptides derived from DRiPs but does not alter, or may even partially diminish, the presentation of peptides undergoing normal protein turnover. The alteration of stable protein accumulation and enhanced DRiP presentation are not the result of TLR stimulation in infected cells, since the treatment of JY/SCRAP-SVG cells for various TLR ligands for 24 h did not impact VFP fluorescence, nor did TLR stimulation result in a statistically significant increase in DRiP presentation (Fig. 3G). Finally, to determine whether this phenotype was restricted to our cell line or is a general feature of chlamydial infection, we infected an epithelial cell line with a clinically prevalent strain of *C. trachomatis*. As shown in Fig. 3H, infection of the human epithelial cell line MCF7 expressing SCRAP-SVG with *C. trachomatis* D/UW-3 resulted in a loss of VFP signal ( $P < 0.01$ ) and an increase in surface HLA-A2-SVG complexes ( $P < 0.05$ , Student *t* test).

*C. trachomatis* infection may alter the host cell in many ways to facilitate enhanced DRiP antigen presentation. We first tested to determine whether the mere presence of the bacterium was sufficient to alter the host cell by treating infected cells with rifampin to block bacterial transcription (Fig. 4A) or with CAM to block bacterial protein synthesis (Fig. 4B) and by measuring SVG peptide presentation in the presence of Shield-1. Treatment with either drug reversed the *Chlamydia*-induced presentation of DRiP-derived peptides (Fig. 4A and B,  $P < 0.05$ ). These data suggest that the growth of the bacteria was necessary to alter the host cell and that the skewed peptide presentation was not the result of materials present in the infectious inoculum. One feature shared between *C. trachomatis* and *C. caviae* is the genus-common chlamydial lipooligosaccharide (LOS). To determine whether LOS

may be responsible for enhancing DRiP-presentation, we treated infected cells with LPC-011 (LPC) to inhibit the synthesis of chlamydial LOS. LPC successfully prevented the accumulation of LOS in infected cells (Fig. 4C) but did not prevent *C. trachomatis* genome replication, as determined by qPCR (Fig. 4D). LPC treatment partially reversed the enhanced DRiP presentation induced by *C. trachomatis* infection (Fig. 4E), returning the levels of the HLA-A2-SVG peptide complexes to levels similar to those in uninfected cells, indicating that LOS may be responsible for altering the cellular antigen presentation machinery.

Antigen presentation is often dependent on proteasomes, which degrade precursor proteins (from both DRiP or non-DRiP sources) into antigenic peptides or peptide-precursors. To determine whether SCRAP-SVG was degraded in a proteasome-dependent process, we treated cells with Shield-1 overnight and, the following day, washed the cells in complete medium and cultured cells in the absence of Shield-1 while monitoring the VFP levels. The degradation of SCRAP-SVG is mediated by the proteasome (Fig. 5A), since the removal of Shield-1 from the cells resulted in the loss of VFP signal, which can be blocked by the proteasome inhibitor epoxomicin. Interestingly, SCRAP-SVG synthesis also requires a functional proteasome. JY/SCRAP-SVG cells were treated with Shield-1 and either DMSO or epoxomicin, and VFP fluorescence was monitored over time. VFP signal increased in cells treated with DMSO, but in the presence of epoxomicin the VFP signal began to plateau after 2 h of treatment with Shield-1 (Fig. 5B). This indicates a defect in either global protein synthesis or SCRAP-SVG specific synthesis due to proteasome inhibition, as has been previously observed for certain proteins (30). The degradation of previously stabilized SCRAP-SVG molecules could yield peptides for antigen presentation. To test this, cells were

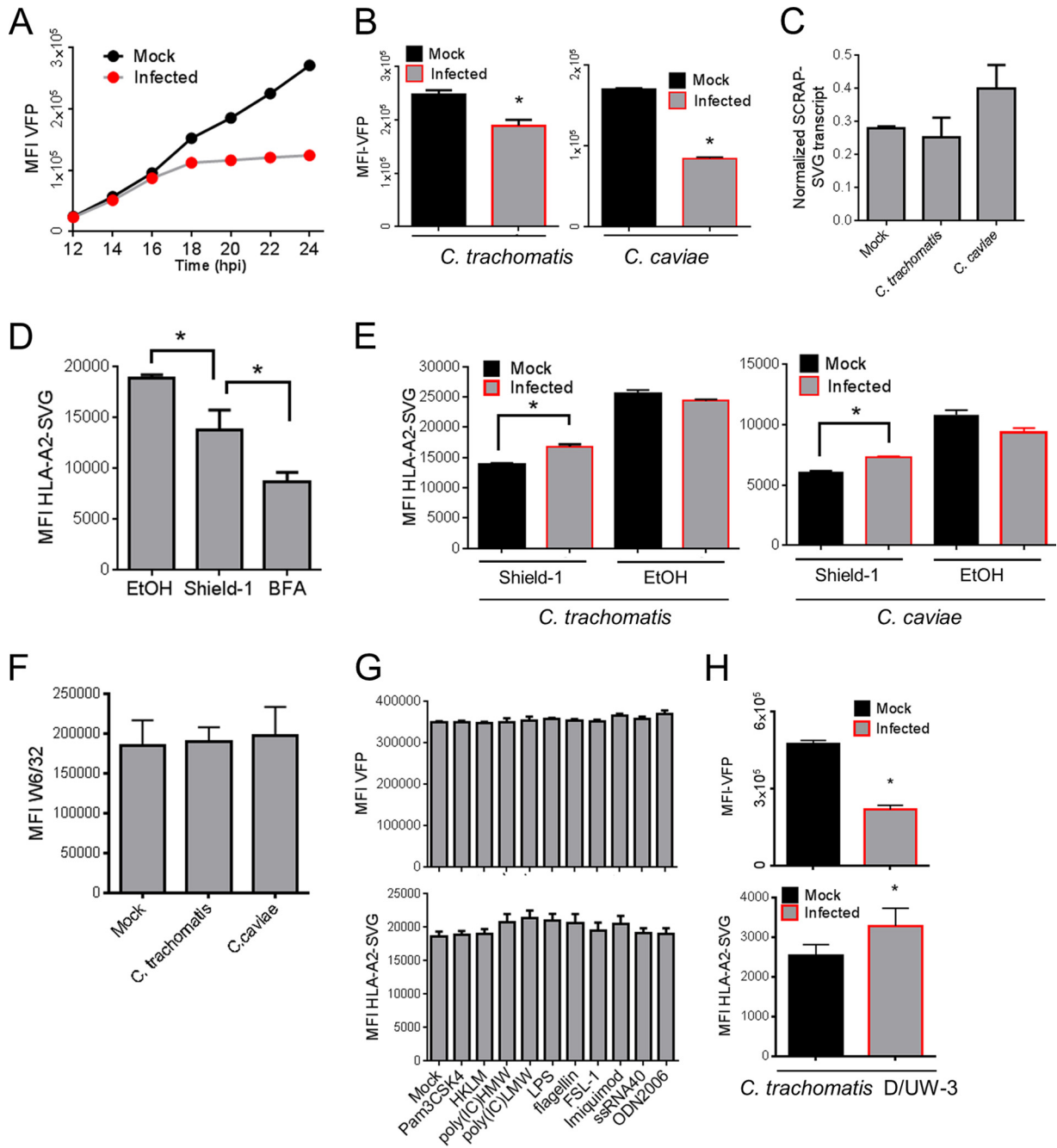


**FIG 3** *Chlamydia* infection prevents accumulation of SCRAP-SVG while enhancing presentation of the SVG peptide. (A) JY/SCRAP-SVG cells were infected with RFP-expressing *C. trachomatis* and cultured for 12 h prior to the addition of Shield-1. VFP fluorescence was monitored over the next 12 h, and the MFI was plotted. (B) JY/SCRAP-SVG cells were infected with either *C. trachomatis* or *C. caviae* and cultured for 12 h before the addition of 1.0  $\mu$ M Shield-1. The cells were cultured for an additional 12 h and analyzed in triplicate by flow cytometry for VFP expression. VFP fluorescence was significantly decreased ( $P < 0.05$ ) for infected cells. (C) JY/SCRAP-SVG cells were mock infected or infected with either *C. trachomatis* or *C. caviae*, and 24 hpi, mRNA was extracted from cells and used to synthesize cDNA. SCRAP-SVG transcripts were quantified by qPCR. (D) JY/SCRAP-SVG cells were treated with EtOH, Shield-1, or BFA for 12 h, and the HLA-A2-SVG complexes were quantified. Results seen with Shield-1 treatment were significantly different from results for both EtOH- and BFA-treated cells (\*,  $P < 0.05$ ). (E) JY/SCRAP-SVG cells were infected and treated with Shield-1 or ethanol as described for panel B, and HLA-A2-SVG complexes were detected by staining with the RL15A MAb. Shield-1-treated infected cells had significantly more peptide-MHC complexes (\*,  $P < 0.05$ ) than uninfected cells. (F) Total MHC class I was quantified by flow cytometry in both mock-infected and infected cells. (G) JY/SCRAP-SVG cells were treated with the indicated TLR ligands (x axis) for 12 h and Shield-1 for an additional 12 h. The cells were analyzed for VFP expression (top) and HLA-A2-SVG (bottom). No statistically significant changes were noted when TLR-stimulated cells were compared to untreated cells. (H) MCF7 cells were transiently transfected with SCRAP-SVG, infected with *C. trachomatis* serovar D/UW-3, and treated with Shield-1 12 hpi. The cells were analyzed 15 h later by gating on VFP<sup>+</sup> cells, and the average MFI of both the Venus fluorescence and HLA-A2 staining on VFP<sup>+</sup> cells is depicted (\*,  $P < 0.05$ ).

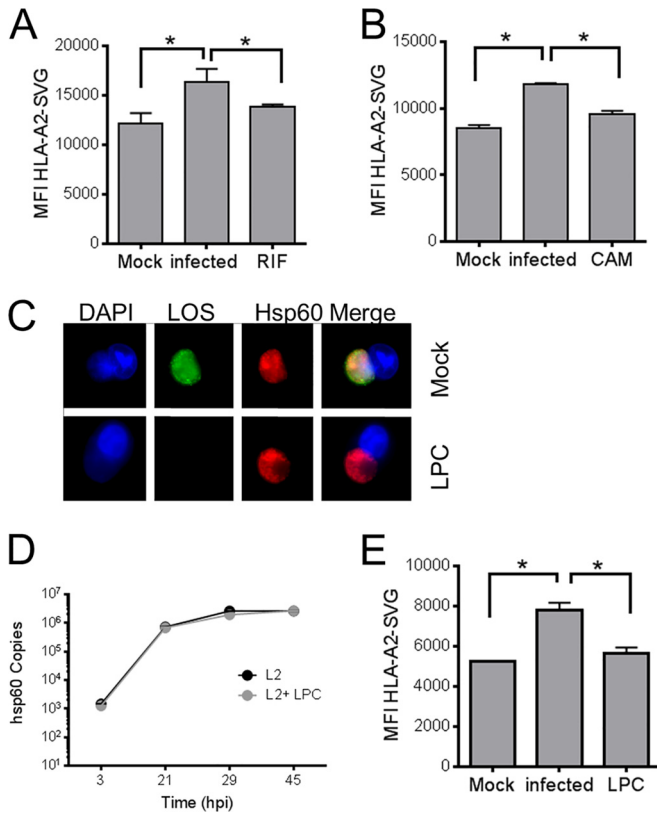


**FIG 4** *C. trachomatis* protein synthesis and LOS are necessary for skewing peptide presentation. Infected and mock-infected JY/SCRAP-SVG cells were treated with RIF (A) or CAM (B) immediately after infection, Shield-1 was added 12 hpi, and HLA-A2-SVG levels were measured 24 hpi. (C) JY/SCRAP-SVG cells were infected with *C. trachomatis* and treated with LPC. After 24 h, the cells were visualized using fluorescence microscopy with antibodies to LOS and bacterial Hsp60. Images of a representative cell from treated and nontreated cells are shown. (D) Cells were treated as described for panel C, and DNA was extracted from cells 24 hpi to determine the *C. trachomatis* genome copy number by qPCR. (E) JY/SCRAP-SVG cells were infected and treated with LPC or left untreated and then exposed to Shield-1, and HLA-A2-SVG complexes were quantified by RL15A staining at 24 hpi. Results for LPC-treated cells are significantly different from results for untreated, infected cells (\*,  $P < 0.05$ ).

treated with either Shield-1 or an ethanol control overnight and were subsequently acid washed to remove existing peptide-MHC complexes. After the loss of Shield-1 from cells, an increase in peptide presentation can be detected (Fig. 5C) as SCRAP-SVG “retired” by the cells is degraded into peptides. To determine whether the presentation was mediated by the proteasome, we treated cells with epoxomicin. Epoxomicin blocked presentation of peptides from both retired SCRAP-SVG (measured in cells upon the loss of Shield-1) and newly synthesized and destabilized SCRAP-SVG (Fig. 5C). To determine whether the loss of SCRAP-SVG in bacterium-infected cells was due to proteasome-mediated degradation, we treated uninfected or *C. caviae*-infected cells with epoxomicin at 24 hpi for a 2-h time period in the presence of Shield-1. Proteasome inhibition failed to rescue VFP fluorescence (Fig. 5D).

Fluorescent proteins require proper folding in order for the fluorochrome to function. To test whether the loss of SCRAP-SVG fluorescence was due to improper protein folding, we analyzed total cell lysates of infected and mock-infected cells treated with Shield-1 and epoxomicin by Western blot analysis. The levels

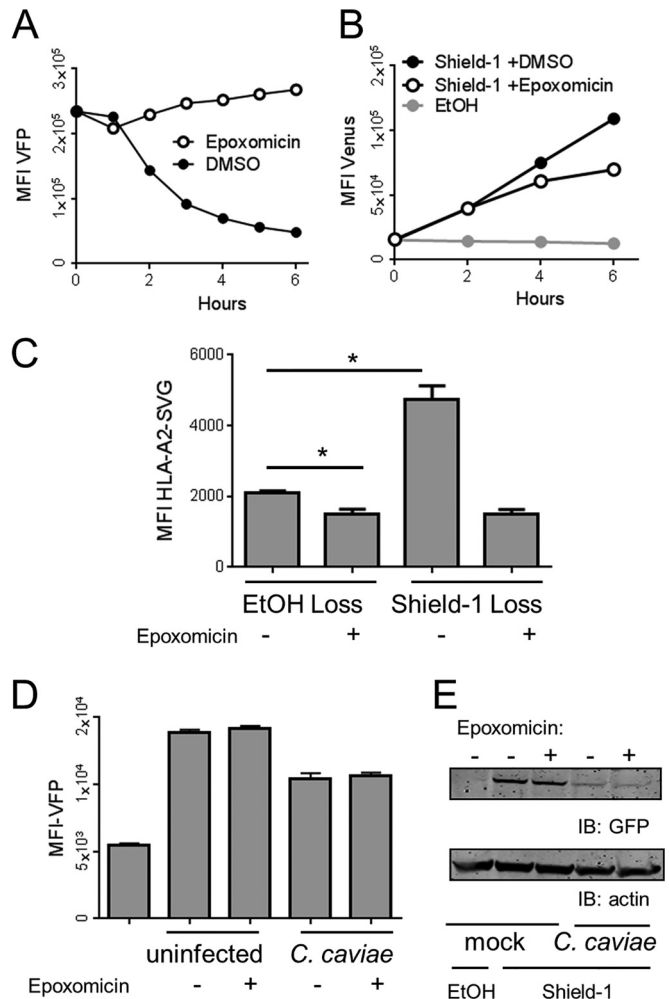


**FIG 5** Chlamydia-induced loss of SCRAP-SVG is not mediated by proteasomal degradation. (A) JY/SCRAP-SVG cells were cultured overnight in the presence of Shield-1, and the following day, the cells were washed and cultured in the absence of Shield-1 but in the presence of epoxomicin or DMSO. VFP fluorescence was monitored at the indicated times. (B) JY/SCRAP-SVG cells were cultured with Shield-1 plus epoxomicin or with Shield-1 alone, and VFP accumulation was monitored at the indicated times. (C) JY/SCRAP-SVG cells were treated with Shield-1 or EtOH overnight. Existing peptide-MHC complexes were removed by a brief acid wash, and cells were cultured for 2 h in the presence or absence of the proteasome inhibitor epoxomicin. SVG-peptide presentation after Shield-1 “loss” was significantly different than that after the loss of ethanol or in cells treated with epoxomicin (\*,  $P < 0.05$ ). (D and E) *C. caviae*-infected cells were treated with Shield-1 and epoxomicin for 2 h starting at 20 hpi and analyzed for VFP fluorescence (D) or for SCRAP-SVG accumulation by Western blotting (E).

of SCRAP-SVG were diminished in infected cells and did not recover to uninfected levels upon proteasome inhibition (Fig. 5E). Therefore, the lack of SCRAP-SVG accumulation, either in its functionally folded form or in its nonfluorescent state, in chlamydia-infected cells is not due to proteasome-mediated degradation.

The SCRAP system can be used to measure the efficiency of self-antigen presentation, that is, the number of peptides bound to MHC molecules from a defined pool of degraded substrates (19, 24, 31–33). Two measurements are needed to calculate the efficiency: (i) the number of peptide-MHC complexes created from

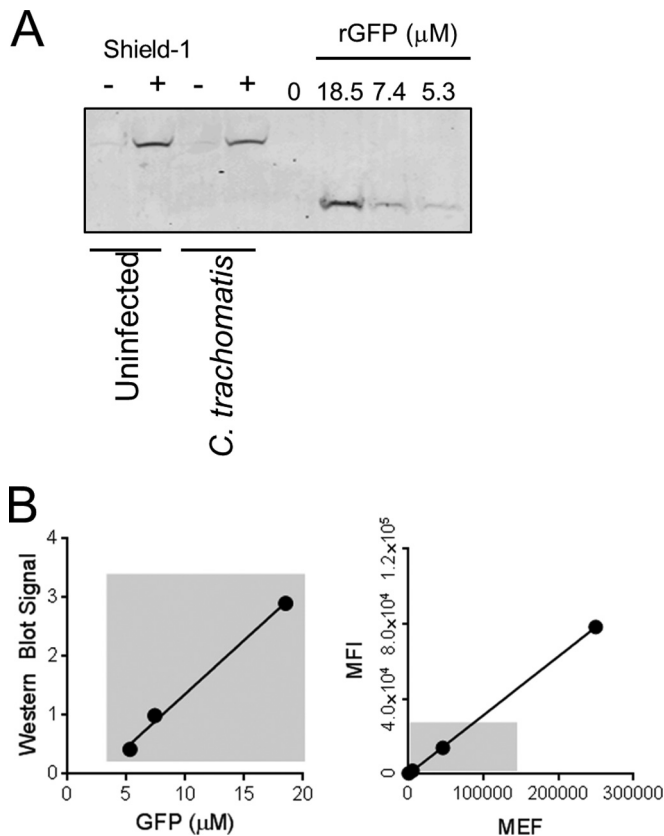


**FIG 6** Quantitative Western blot analysis can be used to calculate loss of SCRAP-SVG induced by *Chlamydia* infection. (A) Representative quantitative Western blot of JY/SCRAP-SVG total cell lysates from cells treated with Shield-1 or ethanol that were either infected or uninfected. Recombinant GFP (rGFP) standards, prepared in lysates of JY cells that do not express SCRAP-SVG, are included on the blot. (B) Standard curves for quantification of GFP (left) and antibody staining (right) are shown. Signal detected by Western blotting is plotted as a function of GFP concentration. For antibody staining, latex beads with known molar equivalents of fluorescent dye (MEF) were analyzed by flow cytometry, and their corresponding MFI is plotted. The shaded region in each plot represents the range of signals detected in each experiment.

(ii) a defined number of precursor proteins that were degraded. The number of peptide-MHC complexes can be measured using quantitative flow cytometry (23), and the number of protein molecules degraded is determined by quantitative Western blotting. Figure 6A shows a sample Western blot comparing untreated and Shield-1-treated cells, infected or not infected with *C. trachomatis*. Membranes were stained for SCRAP-SVG using a goat polyclonal antibody that recognizes a conserved peptide sequence present in both GFP and VFP. Also shown on the blot is commercially available recombinant GFP of various concentrations. A standard curve for the signal of GFP is plotted as a function of concentration (Fig. 6B) and used to determine the molar concentration of VFP in our samples, which in turn can be used to calculate the average number of SCRAP-SVG molecules in each cell. We first computed the efficiency of SVG-peptide presentation by comparing Shield-1-treated and untreated cells in the absence of infection. Dividing the number of HLA-A2-SVG complexes lost due to Shield-1 stabilization of SCRAP-SVG by the total number of SCRAP-SVG molecules generated per cell allows us to determine the efficiency. The results of five matched experiments are pre-

sented in Table 1, and the efficiency of antigen presentation was calculated to be 0.14%, or 1 pMHC generated for approximately every 700 molecules of SCRAP-SVG degraded. Because *Chlamydia* infection increased the number of self-peptide MHC complexes, we suspected the efficiency of antigen presentation may have been altered by infection. We therefore compared Shield-1-treated *C. trachomatis*-infected cells and uninfected cells to determine the efficiency of presentation induced by chlamydial infection, that is, the number of SCRAP-SVG molecules lost as a result of infection and the resulting gain in peptide-MHC complexes. The efficiency of presentation was calculated to be 0.20% (1 pMHC for every 500 molecules lost to infection). There was no significant difference between the efficiencies of presentation from normal protein turnover or induced by *C. trachomatis* infection. Therefore, the elevated level of self-peptide-MHC complexes resulting from *C. trachomatis* infection is not due to an alteration of the efficiency of antigen presentation.

## DISCUSSION

Viruses and intracellular bacteria face a selective pressure to circumvent the adaptive immune responses and can use numerous tactics to evade cytotoxic T cells. The mechanisms used to alter immune responses can provide insights about cellular biology. For example, the importance of cryptic epitopes in antiviral T cell responses (34, 35) and the control of MHC degradation by ubiquitin ligases (36) are but a few instances of how viruses can educate researchers on important elements necessary for successful adaptive immune responses. Here, we found that obligate intracellular bacteria from the *Chlamydia* genus alter the presentation of host-derived peptides during the course of infection. Interestingly, the enhanced levels of peptides are derived from DRiPs, suggesting that the bacteria either actively enhance the generation of DRiPs or increase the rate at which DRiPs are presented. DRiP presentation may be compartmentalized in some manner to ensure efficient antigen presentation (20). Several different potential “compartmental” models have been proposed, including specialized ribosomes (37) and the translation of DRiPs in the nucleus of cells (38–40). Our data suggest that perhaps *Chlamydia* spp. may have evolved to recognize and exploit this process. How this is advantageous to the bacteria is unknown, but it may mask the presence

**TABLE 1** Efficiency of SVG-peptide presentation from SCRAP-SVG precursors

No. of HLA-A2-SVG complexes	No. of SCRAP-SVG molecules	Efficiency (%)
<b>Mock infected</b>		
1,573	1,161,286	0.14
1,387	726,123	0.19
503	649,571	0.08
998	539,140	0.19
1,452	1,121,033	0.13
Avg (mean ± SD)		0.14 ± 0.11
<b><i>C. trachomatis</i> infected</b>		
628	1,081,210	0.06
767	455,847	0.17
1,199	413,277	0.30
513	156,199	0.33
381	247,285	0.15
Avg (mean ± SD)		0.20 ± 0.05

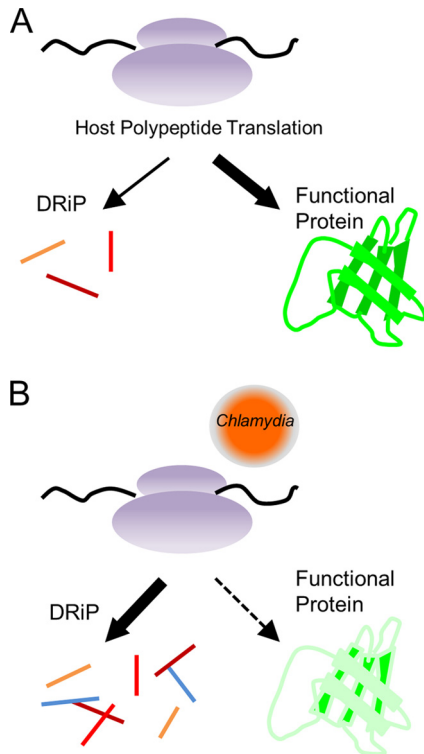


**FIG 7** Model of altered DRiP antigen presentation induced by *Chlamydia* infection. (A) Synthesis of self-proteins on host ribosomes results in the formation of a functional protein or the creation of a DRiP, and this balance exists in some proportion. (B) Upon infection with *Chlamydia*, a bacterium-derived product shifts the balance of host protein synthesis to favor the generation of DRiPs at the expense of stable protein generation, resulting in an increased level of host-derived peptides from the rapidly degraded DRiP fraction.

of infection from the adaptive immune system. If MHC class I molecules bind to more self-peptides derived from DRiPs, it follows that fewer MHC molecules could bind to chlamydia-derived peptides. Although alterations to the MHC-bound peptidome are not uncommon after viral infection, it is not known whether this is due to alteration in the host proteome of the cell or whether it is mediated by enhancing presentation derived from newly synthesized and defective forms of the protein.

Our current model is summarized in Fig. 7. During host-protein synthesis, a fraction of proteins synthesized will have the characteristics of a DRiP, a protein which cannot achieve the function for which it was intended and would be rapidly degraded. The fraction of nascent protein that qualifies as a DRiP has been estimated to be anywhere from 1 to 30% (41), but at this time we do not have an estimate for DRiP generation in our system. We do suspect that the DRiP fraction is small, as Western blot analysis of cells treated with Shield-1 and epoxomicin does not show an appreciable increase in SCRAP-SVG proteins compared to the level in Shield-1-treated cells without proteasome inhibition (Fig. 5E). Even though the fraction of DRiPs is small and not detected biochemically, a measurable level of peptide-MHC complexes can still be generated from this pool of DRiPs, a finding consistent with our previous observations (21). After infection, the levels of VFP detected either by fluorescence (Fig. 3A) or by Western blotting (Fig. 5) stabilize and cannot be rescued by inhibiting proteasome-mediated degradation. Our efforts to determine how much protein

was degraded were hampered by side effects of proteasome inhibition, namely, the impact epoxomicin treatment had on SCRAP-SVG synthesis (Fig. 5B), which limits treatment time to 2 h. Even in this limited window of time, we still could not detect the rescue of SCRAP-SVG by proteasome inhibition. One possible explanation could be that the host cell has stopped synthesizing SCRAP-SVG. However, the presentation of SVG peptides derived from DRiP substrates is increased, which is not consistent with a protein synthesis shutoff. These data suggest that after infection the balance between DRiP and non-DRiP synthesis shifts and favors generation of DRiP substrates and that this results in a corresponding increase in peptide presentation, while stable protein accumulation ceases.

While our data suggest a novel method for controlling antigen presentation during intracellular infections, it is worth considering the limitations of the model system. Shield-1-sensitive fusion proteins offered unparalleled posttranslational control over a particular substrate; however, they are model proteins, and it is unknown whether *Chlamydia* infections happen to target elements of these fusion proteins or DRiPs in general. While *in vitro* experiments have demonstrated that cells of hematopoietic origin, such as dendritic cells and macrophages (42, 43), can be infected with different *Chlamydia* species, epithelial cells are the primary target of infections *in vivo* and antigenic peptides derived from DRiPs are present in different amounts depending on the cell type (44). However, the phenomenon is not limited to JY cells, since an epithelial cell line transiently transfected with SCRAP-SVG also increased DRiP presentation, while stable protein accumulation was diminished (Fig. 3H). Importantly, we used a serovar of *C. trachomatis*, D/UW-3, which is more prevalent in clinical infections than serovar L2.

Chlamydial infections are often associated with the development of autoimmune disorders such as reactive arthritis (ReA), atherosclerosis, and others (16, 45, 46). ReA is strongly correlated with the expression of a particular MHC class I allele, HLA-B27 (47–49). Animal models have shown that chlamydia-reactive CD8<sup>+</sup> T cells can recognize self-peptides bound to HLA-B27 (50–52). Since self-reactive CD8<sup>+</sup> T cells are known to induce autoimmune diseases (53) through the recognition of self-peptide MHC complexes (54–56), it is possible that an increase in self-antigen presentation during chlamydial infections may drive autoimmune diseases.

Intracellular pathogens often alter the host cell proteome, which can be attributed either to the host attempting to fight off the infection or to the pathogen enhancing the cellular environment to complete its replication. Many times, this manifests itself in alterations to the transcriptome, which have been observed for a variety of *Chlamydia* species (57–59). However, a recent report demonstrated that *C. trachomatis* infection can alter the abundance of host proteins without altering levels of transcripts (60). In this way the bacterium was able to stabilize host components necessary for its survival. Similar to our findings here (Fig. 3C), the levels of other proteins were diminished without appreciable alterations to the transcript levels (60). Future work will be needed to determine whether *C. trachomatis* reduces particular host proteins either because they are detrimental to the bacteria or simply because they provide self-peptides for antigen presentation, as demonstrated here.

How *C. trachomatis* evades the CD8<sup>+</sup> T cell response is largely unknown. Similar to several herpesviruses, modest decreases in total MHC class I expression have been reported in cells infected

with a variety of *Chlamydia* species (7–9), but this does not always occur (61), consistent with our reported data (see Fig. 3F). Although suppression of MHC class I levels may be advantageous for preventing presentation of chlamydial peptides, it might render cells susceptible to NK cell-mediated killing. Indeed, Ibana et al. report that modulation of the MHC class I-like molecule MICA can render *C. trachomatis*-infected epithelial cells targets of NK cell killing (62). Although we and others suppose that alterations of the MHC class I pathway may help bacteria evade cytotoxic T cell responses, the results cannot be absolute, since multiple peptide determinants have been identified and reactive T cells have been detected in patients. Multiple pathways are likely used to evade cytotoxic T cell responses, such as the recent finding by Fankhauser and Starnbach that chlamydial infections result in increased expression of the immunoinhibitory ligand PD-L1 (63). Future research is likely to determine even more ways in which chlamydiae evade the adaptive immune response.

## ACKNOWLEDGMENTS

We thank Robert J. Suchland of the University of Washington for the *Chlamydia trachomatis* serovar L2 strain expressing RFP. We also thank Bishop Hague and the National Institute of Allergy and Infectious Diseases Research Technologies Branch Flow Cytometry Section for expert cell sorting. LPC-011 was a kind gift of Pei Zhou and Raphael Valdivia of Duke University. We also thank the Oregon State University Electron Microscopy Facility.

## FUNDING INFORMATION

HHS | National Institutes of Health (NIH) provided funding to Brian P. Dolan under grant number K22AI089861. HHS | National Institutes of Health (NIH) provided funding to Brian P. Dolan under grant number R56AI112588.

The funders had no role in study design, data collection and interpretation, or the decision to submit the work for publication.

## REFERENCES

- Wizel B, Nyström-Asklin J, Cortes C, Tvinnereim A. 2008. Role of CD8<sup>+</sup> T cells in the host response to *Chlamydia*. *Microbes Infect* 10:1420–1430. <http://dx.doi.org/10.1016/j.micinf.2008.08.006>.
- Holland MJ, Faal N, Sarr I, Joof H, Laye M, Cameron E, Pemberton-Pigott F, Dockrell HM, Bailey RL, Mabey DCW. 2006. The frequency of *Chlamydia trachomatis* major outer membrane protein-specific CD8<sup>+</sup> T lymphocytes in active trachoma is associated with current ocular infection. *Infect Immun* 74:1565–1572. <http://dx.doi.org/10.1128/IAI.74.3.1565-1572.2006>.
- Kim S-K, Devine L, Angevine M, DeMars R, Kavathas PB. 2000. Direct detection and magnetic isolation of *Chlamydia trachomatis* major outer membrane protein-specific CD8<sup>+</sup> CTLs with HLA class I tetramers. *J Immunol* 165:7285–7292. <http://dx.doi.org/10.4049/jimmunol.165.12.7285>.
- Darville T, Hiltke TJ. 2010. Pathogenesis of genital tract disease due to *Chlamydia trachomatis*. *J Infect Dis* 201:S114–S125.
- Hansen TH, Bouvier M. 2009. MHC class I antigen presentation: learning from viral evasion strategies. *Nat Rev Immunol* 9:503–513. <http://dx.doi.org/10.1038/nri2575>.
- Baena A, Porcelli SA. 2009. Evasion and subversion of antigen presentation by *Mycobacterium tuberculosis*. *Tissue Antigens* 74:189–204. <http://dx.doi.org/10.1111/j.1399-0039.2009.01301.x>.
- Caspar-Bauguil S, Puissant B, Nazzari D, Lefevre JC, Thomsen M, Salvayre R, Benoist H. 2000. *Chlamydia pneumoniae* induces interleukin-10 production that down-regulates major histocompatibility complex class I expression. *J Infect Dis* 182:1394–1401. <http://dx.doi.org/10.1086/315856>.
- Ibana JA, Schust DJ, Sugimoto J, Nagamatsu T, Greene SJ, Quayle AJ. 2011. *Chlamydia trachomatis* immune evasion via downregulation of MHC class I surface expression involves direct and indirect mechanisms. *Infect Dis Obstet Gynecol* 2011:420905.
- Zhong G, Liu L, Fan T, Fan P, Ji H. 2000. Degradation of transcription factor Rfx5 during the inhibition of both constitutive and interferon  $\gamma$ -inducible major histocompatibility complex class I expression in *Chlamydia*-infected cells. *J Exp Med* 191:1525–1534. <http://dx.doi.org/10.1084/jem.191.9.1525>.
- Hickman HD, Luis AD, Bardet W, Buchli R, Battson CL, Shearer MH, Jackson KW, Kennedy RC, Hildebrand WH. 2003. Cutting edge: class I presentation of host peptides following HIV infection. *J Immunol* 171:22–26. <http://dx.doi.org/10.4049/jimmunol.171.1.22>.
- Herberts CA, van Gaans-van den Brink J, van der Heeft E, van Wijk M, Hoekman J, Jaye A, Poelen MC, Boog CJ, Roholl PJ, Whittle H, de Jong AP, van Els CA. 2003. Autoreactivity against induced or upregulated abundant self-peptides in HLA-A\*0201 following measles virus infection. *Hum Immunol* 64:44–55. [http://dx.doi.org/10.1016/S0198-8859\(02\)00707-3](http://dx.doi.org/10.1016/S0198-8859(02)00707-3).
- Wahl A, Schafer F, Bardet W, Hildebrand WH. 2010. HLA class I molecules reflect an altered host proteome after influenza virus infection. *Hum Immunol* 71:14–22. <http://dx.doi.org/10.1016/j.humimm.2009.08.012>.
- Meiring HD, Soethout EC, Poelen MCM, Mooibroek D, Hoogerbrugge R, Timmermans H, Boog CJ, Heck AJR, de Jong AP, van Els CA. 2006. Stable isotope tagging of epitopes: a highly selective strategy for the identification of major histocompatibility complex class I-associated peptides induced upon viral infection. *Mol Cell Proteomics* 5:902–913.
- Caron E, Vincent K, Fortier MH, Laverdure JP, Bramoullé A, Hardy MP, Voisin G, Roux PP, Lemieux S, Thibault P, Perreault C. 2011. The MHC I immunopeptidome conveys to the cell surface an integrative view of cellular regulation. *Mol Syst Biol* 7:533. <http://dx.doi.org/10.1038/msb.2011.68>.
- Bachmaier K, Penninger JM. 2005. Chlamydia and antigenic mimicry, p 153–163. In Oldstone MA (ed), *Molecular mimicry: infection-inducing autoimmune disease*, vol 296. Springer, Berlin, Germany.
- Girschick HJ, Guilherme L, Inman RD, Latsch K, Rühl M, Sherer Y, Shoenfeld Y, Zeidler H, Arienti S, Doria A. 2008. Bacterial triggers and autoimmune rheumatic diseases. *Clin Exp Rheumatol* 26:S12–S17.
- Palmer AL, Dolan BP. 2013. MHC class I antigen presentation of DR1p-derived peptides from a model antigen is not dependent on the AAA ATPase p97. *PLoS One* 8:e67796. <http://dx.doi.org/10.1371/journal.pone.0067796>.
- Kim S, Li L, McMurtrey CP, Hildebrand WH, Weidanz JA, Gillanders WE, Diamond MS, Hansen TH. 2010. Single-chain HLA-A2 MHC trimers that incorporate an immunodominant peptide elicit protective T cell immunity against lethal West Nile virus infection. *J Immunol* 184:4423–4430. <http://dx.doi.org/10.4049/jimmunol.0903955>.
- Dolan BP, Sharma AA, Gibbs JS, Cunningham TJ, Bennink JR, Yewdell JW. 2012. MHC class I antigen processing distinguishes endogenous antigens based on their translation from cellular vs. viral mRNA. *Proc Natl Acad Sci U S A* 109:7025–7030. <http://dx.doi.org/10.1073/pnas.1112387109>.
- Lev A, Princiotta MF, Zanker D, Takeda K, Gibbs JS, Kumagai C, Waffarn E, Dolan BP, Burgevin A, Van Ender P, Chen W, Bennink JR, Yewdell JW. 2010. Compartmentalized MHC class I antigen processing enhances immunosurveillance by circumventing the law of mass action. *Proc Natl Acad Sci U S A* 107:6964–6969. <http://dx.doi.org/10.1073/pnas.0910997107>.
- Dolan BP, Li L, Veltri CA, Ireland CM, Bennink JR, Yewdell JW. 2011. Distinct pathways generate peptides from defective ribosomal products for CD8<sup>+</sup> T cell immunosurveillance. *J Immunol* 186:2065–2072. <http://dx.doi.org/10.4049/jimmunol.1003096>.
- Sandoz KM, Valiant WG, Eriksen SG, Hrubby DE, Allen RD, Rockey DD. 2014. The broad-spectrum antiviral compound ST-669 restricts chlamydial inclusion development and bacterial growth and localizes to host cell lipid droplets within treated cells. *Antimicrob Agents Chemother* 58:3860–3866. <http://dx.doi.org/10.1128/AAC.02064-13>.
- Dolan BP. 2013. Quantitating MHC class I ligand production and presentation using TCR-like antibodies. *Methods Mol Biol* 960:169–177. [http://dx.doi.org/10.1007/978-1-62703-218-6\\_14](http://dx.doi.org/10.1007/978-1-62703-218-6_14).
- Princiotta MF, Finzi D, Qian SB, Gibbs J, Schuchmann S, Buttgerit F, Bennink JR, Yewdell JW. 2003. Quantitating protein synthesis, degradation, and endogenous antigen processing. *Immunity* 18:343–354. [http://dx.doi.org/10.1016/S1074-7613\(03\)00051-7](http://dx.doi.org/10.1016/S1074-7613(03)00051-7).
- Banaszynski LA, Chen L-C, Maynard-Smith LA, Ooi AG, Wandless TJ. 2006. A rapid, reversible, and tunable method to regulate protein function in living cells using synthetic small molecules. *Cell* 126:995–1004. <http://dx.doi.org/10.1016/j.cell.2006.07.025>.
- Fiebigler BM, Moosmann A, Behrends U, Mautner J. 2012. Mature proteins derived from Epstein-Barr virus fail to feed into the MHC class I

- antigenic pool. *Eur J Immunol* 42:3167–3173. <http://dx.doi.org/10.1002/jei.201242627>.
27. Yewdell JW, Anton LC, Bennink JR. 1996. Defective ribosomal products (DRiPs): a major source of antigenic peptides for MHC class I molecules? *J Immunol* 157:1823–1826.
  28. Dolan BP, Bennink JR, Yewdell JW. 2011. Translating DRiPs: progress in understanding viral and cellular sources of MHC class I peptide ligands. *Cell Mol Life Sci* 68:1481–1489. <http://dx.doi.org/10.1007/s00018-011-0656-z>.
  29. Yewdell JW. 2011. DRiPs solidify: progress in understanding endogenous MHC class I antigen processing. *Trends Immunol* 32:548–558. <http://dx.doi.org/10.1016/j.it.2011.08.001>.
  30. Milner E, Gutter-Kapon L, Bassani-Strenberg M, Barnea E, Beer I, Admon A. 2013. The effect of proteasome inhibition on the generation of the human leukocyte antigen (HLA) peptidome. *Mol Cell Proteomics* 12:1853–1864.
  31. Wolf BJ, Princiotta MF. 2013. Processing of recombinant *Listeria monocytogenes* proteins for MHC class I presentation follows a dedicated, high-efficiency pathway. *J Immunol* 190:2501–2509. <http://dx.doi.org/10.4049/jimmunol.1201660>.
  32. Villanueva MS, Beckers CJ, Pamer EG. 1994. Infection with *Listeria monocytogenes* impairs sialic acid addition to host cell glycoproteins. *J Exp Med* 180:2137–2145. <http://dx.doi.org/10.1084/jem.180.6.2137>.
  33. Villanueva MS, Sijts AJ, Pamer EG. 1995. Listeriolysin is processed efficiently into an MHC class I-associated epitope in *Listeria monocytogenes*-infected cells. *J Immunol* 155:5227–5233.
  34. Bansal A, Carlson J, Yan J, Akinsiku OT, Schaefer M, Sabbaj S, Bet A, Levy DN, Heath S, Tang J, Kaslow RA, Walker BD, Ndung'u T, Goulder PJ, Heckerman D, Hunter E, Goepfert PA. 2010. CD8 T cell response and evolutionary pressure to HIV-1 cryptic epitopes derived from antisense transcription. *J Exp Med* 207:51–59. <http://dx.doi.org/10.1084/jem.20092060>.
  35. Berger CT, Carlson JM, Brumme CJ, Hartman KL, Brumme ZL, Henry LM, Rosato PC, Piechocka-Trocha A, Brockman MA, Harrigan PR, Heckerman D, Kaufmann DE, Brander C. 2010. Viral adaptation to immune selection pressure by HLA class I-restricted CTL responses targeting epitopes in HIV frameshift sequences. *J Exp Med* 207:61–75. <http://dx.doi.org/10.1084/jem.20091808>.
  36. Boname JM, Lehner PJ. 2011. What has the study of the K3 and K5 viral ubiquitin E3 ligases taught us about ubiquitin-mediated receptor regulation? *Viruses* 3:118–131. <http://dx.doi.org/10.3390/v3020118>.
  37. Yewdell JW, Nicchitta CV. 2006. The DRiP hypothesis decennial: support, controversy, refinement, and extension. *Trends Immunol* 27:368–373. <http://dx.doi.org/10.1016/j.it.2006.06.008>.
  38. Apcher S, Millot G, Daskalogianni C, Scherl A, Manoury B, Fähræus R. 2013. Translation of pre-spliced RNAs in the nuclear compartment generates peptides for the MHC class I pathway. *Proc Natl Acad Sci U S A* 110:17951–17956. <http://dx.doi.org/10.1073/pnas.1309956110>.
  39. David A, Dolan BP, Hickman HD, Knowlton JJ, Clavarino G, Pierre P, Bennink JR, Yewdell JW. 2012. Nuclear translation visualized by ribosome-bound nascent chain puromycylation. *J Cell Biol* 197:45–57. <http://dx.doi.org/10.1083/jcb.201112145>.
  40. Dolan BP, Knowlton JJ, David A, Bennink JR, Yewdell JW. 2010. RNA polymerase II inhibitors dissociate antigenic peptide generation from normal viral protein synthesis: a role for nuclear translation in defective ribosomal product synthesis? *J Immunol* 185:6728–6733. <http://dx.doi.org/10.4049/jimmunol.1002543>.
  41. Antón LC, Yewdell JW. 2014. Translating DRiPs: MHC class I immunosurveillance of pathogens and tumors. *J Leukoc Biol* 95:551–562. <http://dx.doi.org/10.1189/jlb.1113599>.
  42. Datta B, Njau F, Thalmann J, Haller H, Wagner AD. 2014. Differential infection outcome of *Chlamydia trachomatis* in human blood monocytes and monocyte-derived dendritic cells. *BMC Microbiol* 14:209. <http://dx.doi.org/10.1186/s12866-014-0209-3>.
  43. Fields KA, McCormack R, de Armas LR, Podack ER. 2013. Perforin-2 restricts growth of *Chlamydia trachomatis* in macrophages. *Infect Immun* 81:3045–3054. <http://dx.doi.org/10.1128/IAI.00497-13>.
  44. Bourdetsky D, Schmelzer CEH, Admon A. 2014. The nature and extent of contributions by defective ribosome products to the HLA peptidome. *Proc Natl Acad Sci U S A* 111:E1591–E1599. <http://dx.doi.org/10.1073/pnas.1321902111>.
  45. Filardo S, Di Pietro M, Farcomeni A, Schiavoni G, Sessa R. 2015. *Chlamydia pneumoniae*-mediated inflammation in atherosclerosis: a meta-analysis. *Mediators Inflamm* 2015:378658. <http://dx.doi.org/10.1155/2015/378658>.
  46. Stratton CW, Wheldon DB. 2006. Multiple sclerosis: an infectious syndrome involving *Chlamydia pneumoniae*. *Trends Microbiol* 14:474–479. <http://dx.doi.org/10.1016/j.tim.2006.09.002>.
  47. Alvarez-Navarro C, Cragolini JJ, Dos Santos HG, Barnea E, Admon A, Morreale A, López de Castro JA. 2013. Novel HLA-B27-restricted epitopes from *Chlamydia trachomatis* generated upon endogenous processing of bacterial proteins suggest a role of molecular mimicry in reactive arthritis. *J Biol Chem* 288:25810–25825. <http://dx.doi.org/10.1074/jbc.M113.493247>.
  48. Dulphy N, Peyrat M-A, Tieng V, Douay C, Rabian C, Tamouza R, Laoussadi S, Berenbaum F, Chabot A, Bonneville M, Charron D, Toubert A. 1999. Common intra-articular T cell expansions in patients with reactive arthritis: identical  $\beta$ -chain junctional sequences and cytotoxicity toward HLA-B27. *J Immunol* 162:3830–3839.
  49. Cragolini JJ, García-Medel N, López de Castro JA. 2009. Endogenous processing and presentation of T-cell epitopes from *Chlamydia trachomatis* with relevance in HLA-B27-associated reactive arthritis. *Mol Cell Proteomics* 8:1850–1859.
  50. Kuon W, Holzhütter H-G, Appel H, Grolms M, Kollnberger S, Traeder A, Henklein P, Weiss E, Thiel A, Lauster R, Bowness P, Radbruch A, Kloetzel P-M, Sieper J. 2001. Identification of HLA-B27-restricted peptides from the *Chlamydia trachomatis* proteome with possible relevance to HLA-B27-associated diseases. *J Immunol* 167:4738–4746. <http://dx.doi.org/10.4049/jimmunol.167.8.4738>.
  51. Kuon W, Lauster R, Bottcher U, Koroknay A, Ulbrecht M, Hartmann M, Grolms M, Ugrinovic S, Braun J, Weiss EH, Sieper J. 1997. Recognition of chlamydial antigen by HLA-B27-restricted cytotoxic T cells in HLA-B\*2705 transgenic CBA (H-2k) mice. *Arthritis Rheum* 40:945–954. <http://dx.doi.org/10.1002/art.1780400524>.
  52. Popov I, Dela Cruz CS, Barber BH, Chiu B, Inman RD. 2001. The effect of an anti-HLA-B27 immune response on CTL recognition of *Chlamydia*. *J Immunol* 167:3375–3382. <http://dx.doi.org/10.4049/jimmunol.167.6.3375>.
  53. Walter U, Santamaria P. 2005. CD8<sup>+</sup> T cells in autoimmunity. *Curr Opin Immunol* 17:624–631. <http://dx.doi.org/10.1016/j.coi.2005.09.014>.
  54. Sorrentino R, Böckmann RA, Fiorillo MT. 2014. HLA-B27 and antigen presentation: at the crossroads between immune defense and autoimmunity. *Mol Immunol* 57:22–27. <http://dx.doi.org/10.1016/j.molimm.2013.06.017>.
  55. Gudjonsson JE, Johnston A, Sigmundsdottir H, Valdimarsson H. 2004. Immunopathogenic mechanisms in psoriasis. *Clin Exp Immunol* 135:1–8.
  56. Roep BO, Peakman M. 2012. Antigen targets of type 1 diabetes autoimmunity. *Cold Spring Harb Perspect Med* 2:a007781. <http://dx.doi.org/10.1101/cshperspect.a007781>.
  57. Alvesalo J, Greco D, Leinonen M, Raitila T, Vuorela P, Auvinen P. 2008. Microarray analysis of a *Chlamydia pneumoniae*-infected human epithelial cell line by use of gene ontology hierarchy. *J Infect Dis* 197:156–162. <http://dx.doi.org/10.1086/524142>.
  58. Schrader S, Klos A, Hess S, Zeidler H, Kuipers J, Rihl M. 2007. Expression of inflammatory host genes in *Chlamydia trachomatis*-infected human monocytes. *Arthritis Res Ther* 9:R54. <http://dx.doi.org/10.1186/ar2209>.
  59. Xia M, Bumgarner RE, Lampe MF, Stamm WE. 2003. *Chlamydia trachomatis* infection alters host cell transcription in diverse cellular pathways. *J Infect Dis* 187:424–434. <http://dx.doi.org/10.1086/367962>.
  60. Olive AJ, Haff MG, Emanuele MJ, Sack LM, Barker JR, Elledge SJ, Starnbach MN. 2014. *Chlamydia trachomatis*-induced alterations in the host cell proteome are required for intracellular growth. *Cell Host Microbe* 15:113–124. <http://dx.doi.org/10.1016/j.chom.2013.12.009>.
  61. Kägebein D, Gutjahr M, Große C, Vogel AB, Rödel J, Knittler MR. 2013. *Chlamydia*-infected epithelial cells and fibroblasts retain the ability to express surface-presented MHC class I molecules. *Infect Immun* 82:993–1006. <http://dx.doi.org/10.1128/IAI.01473-13>.
  62. Ibana JA, Aiyar A, Quayle AJ, Schust DJ. 2012. Modulation of MICA on the surface of *Chlamydia trachomatis*-infected endocervical epithelial cells promotes NK cell-mediated killing. *FEMS Immunol Med Microbiol* 65:32–42. <http://dx.doi.org/10.1111/j.1574-695X.2012.00930.x>.
  63. Fankhauser SC, Starnbach MN. 2014. PD-L1 limits the mucosal CD8<sup>+</sup> T cell response to *Chlamydia trachomatis*. *J Immunol* 192:1079–1090. <http://dx.doi.org/10.4049/jimmunol.1301657>.